C. R. Geoscience 348 (2016) 451–461

Contents lists available at ScienceDirect

Comptes Rendus Geoscience

www.sciencedirect.com

Stratigraphy, Sedimentology

Monitoring of dredged-dumped sediment dispersal off the Bay of the Seine (northern France) using environmental magnetism

Jean Nizou [a,*], François Demory [b], Carole Dubrulle-Brunaud [a]

[a] Caen University, CNRS UMR 6143, Morphodynamique continentale et côtière, 14000 Caen, France
[b] Aix Marseille University, CNRS, IRD, CEREGE UM34, 13545 Aix-en-Provence cedex 04, France

ARTICLE INFO

Article history:
Received 7 October 2014
Accepted after revision 24 February 2015
Available online 30 April 2015

Handled by Slyvie Bourquin

Keywords:
Environmental magnetism
Monitoring dredged-dumped sediment dispersal
Magnetic susceptibility
Sediment fingerprinting
Bay of the Seine

ABSTRACT

In this study, we developed a novel approach for fingerprinting dredged-dumped sediments at sea using magnetic susceptibility. Several magnetic measurements were performed on discrete sedimentary samples from the dredged areas in the Seine River and from the Bay of Seine seafloor before and after dumping. The dredged sediments showed higher susceptibility values than the undisturbed seafloor, which allowed the mapping of the dispersion of dredged-dumped sediments. In the vicinity of the coast and the estuary, high-susceptibility terrestrial input from rivers could also be mapped by this technique, therefore monitoring of the dumping by the susceptibility proxy is limited to the offshore areas. This susceptibility signal is controlled by the ferromagnetic fraction of the sediment. Furthermore, a constant magnetite-dominated magneto-mineralogy is observed in the study area. In addition to the susceptibility, a magnetic grain size parameter of the low-coercive fraction was also found to be sensitive to dumping. Both tracers showed an in progress resilience of the sedimentary environment during a 6-month survey.

1. Introduction

The Bay of the Seine is a strongly anthropogenic environment that displays, among other pollutants, heavy metals (Chiffoleau et al., 1999), trace metals (Meybeck et al., 2007), and PCB contaminations (Chevreuil et al., 1998), as well as several sedimentary disruptions by constructions (Avoine et al., 1981) and boating (Verney et al., 2007). In addition, dredged sediments originating from the coastal harbours and the navigation channels of the Seine are dumped at sea to maintain the necessary water depth for vessel navigation. Disposals of such dredged sediments potentially affect living organisms (Boyd et al., 2003; Cooper et al., 2007; Van der Wal et al., 2011), the water column (Fettweis et al., 2011; Roberts, 2012; Yang et al., 2012), and the sedimentary conditions at the seafloor (Du Four and Van Lancker, 2008; Lepland et al., 2009; Li et al., 2009). Thus, over the last decade, dredge dumping at sea has been monitored by several innovative approaches using natural radionucleides (Venema and de Meijer, 2001), acoustic techniques (Wienberg and Bartholomä, 2005), and particle-size distributions combined with metal concentration analyses (Okada et al., 2009). Besides, environmental magnetism techniques have been used for monitoring heavy metals (Akinyemi et al., 2012; Franke et al., 2009; Pozza et al., 2004), inputs of anthropogenic magnetic spherules (Horng et al., 2009), artificial alpha-radioactivity (McCubbin et al., 2000), as well as petroleum hydrocarbons (Venkatachalapathy et al., 2011) in human-impacted sedimentary systems. However, to our knowledge, no dispersal monitoring of

* Corresponding author.
E-mail address: nizou@uni-bremen.de (J. Nizou).

http://dx.doi.org/10.1016/j.crte.2015.02.005

dredged-dumped spoil sediments has ever been developed using environmental magnetism techniques. It has been recently decided by the Harbour of Rouen (Grand Port Maritime de Rouen) to investigate the impact of two new experimental dumping disposal sites on the sedimentary system of the Bay of the Seine. This study presents a novel application of well-established environmental magnetic proxy parameters calibrated with a magnetic mineralogy study, with the aim to fingerprint and map two experimental dredged-dumped sediment dispersal areas in the Bay of the Seine.

2. Material and methods

2.1. Study area

The Seine river watershed covers a surface of $\sim 65{,}000\ km^2$ (Meybeck et al., 2007) and is almost entirely composed of sedimentary deposits (i.e. Jurassic limestones and terrigenous sediments, Lower Cretaceous sands and marls, Upper Cretaceous chalks, Tertiary limestones and marls), with the exception of its southern tributary, the Yonne River, which drains Hercynian gneissic, granitic and rhyolitic rocks. The watershed is widely covered by Quaternary loess and fluvial deposits (Roy et al., 1999). The Seine River has a length of 780 km and ends in the Bay of the Seine. The sedimentary processes within the estuary are controlled by tidal, wave and river flow dynamics. The Seine River's mean annual flow is $\sim 497\ m^3\ s^{-1}$ (1983–2003) at the Poses station upstream the estuary (Meybeck et al., 2007) and its mean annual mass of suspended particulate matter is $\sim 6{\cdot}10^5$ tons (Lesourd et al., 2003). The tidal range at Le Havre varies from 3 to 7.5 m (Lesourd et al., 2003). The wave regime in the Seine estuary displays the characteristics of sheltered coastlines with low amplitudes (< 3 m) and short periods (3–5 s). Whereas westerly to northwesterly swells prevail, waves generated by local winds also occur with a westerly dominance (Lesourd et al., 2003).

Two sites located within the navigation channel (NC) of the Seine River are regularly dredged by the Harbour of Rouen. Those sites contribute 47% and 53%, respectively, to the total dumping. The dredged sediments are dumped in the Bay of the Seine, off Le Havre, on two experimental disposal sites. On the eastern site, $10^6\ m^3$ of sediments ranging from silts to medium sands were dumped in four steps over a year (i.e. one per season) until February 2013 over a parallelogram area, whereas on the western site, $10^6\ m^3$ of sediments were dumped continuously from May to December 2012 in the form of a cone (Fig. 1A).

2.2. Sampling strategy

Sampling campaigns were performed around the two dumping sites to evaluate sediment dispersal using magnetic proxies (Fig. 1A). The spacing between data points widens away from the two disposal site centres at $\sim 49°27'17''N$, $0°05'26''W$ and $\sim 49°27'33''N$, $0°07'50''W$, up to the adjacent coastal and estuary areas to the south and the east. Offshore sampling reached Octeville latitude to the north and Courseulles-sur-Mer's longitude to the west. In the study area, the water depth ranges between ~ 10 and 20 m. Four sampling campaigns of ~ 142 samples each (the sample number may vary slightly depending on the survey campaigns) were performed: one before dumping to determine the sedimentological background (t_0, from June to September 2011), and three after dumping (t_1, immediately after the last dumping in March 2013; t_2, 3 months after the last dumping in June 2013; t_3 six months after the last dumping in September 2013). The discussion mainly focuses on the offshore part of our study area, which is located within and around the disposal sites (CBS; ~ 122 samples). For comparison with the sediments of the Bay of the Seine, five samples from each of the two dredging sites were retrieved. Sampling was performed using a Shipek grab with a penetration of ~ 10 cm. For comparison, four Reyneck box cores with minimum sediment surface disturbance were retrieved at different time intervals to assess whether some sediment is likely to be resuspended during sampling: before dumping in February 2012, during dumping in November 2012, immediately after the last dumping in March 2013, and 2 months after the last dumping in May 2013.

2.3. Rock magnetism (storage, preparation and measurements)

After retrieval and before further laboratory preparations, the samples were stored in fully filled plastic boxes and kept at 4 °C to minimize post-retrieval oxidation or post-sampling mineral formation. To establish the methodology for sample preparation, a comparison was conducted between 24 wet and dry sample susceptibilities to determine the extent to which diamagnetic water participates to the signal, and to test if the oxidation process that occurs during the drying affects the measurements (data available on http://doi.pangaea.de/10.1594/PANGAEA.830208). No significant change was observed. Therefore, all samples were dried at 40 °C using a drying oven. Afterwards, samples were homogenized using an agate mortar and pestle to avoid metal contamination. Subsequently, the samples were transferred into 6.8-cm^3 plastic cubes.

Rock magnetic analyses were conducted in the magnetic laboratory of the CEREGE institute (Aix-en-Provence, France; the data are available on http://doi.pangaea.de/10.1594/PANGAEA.830212). Rock magnetic measurements were carried out with the aim to trace the sediments dredged from the Seine navigation channel after dumping offshore. The low-field magnetic susceptibility of the samples was measured with an MFK1 AGICO susceptibilimeter. The measurements were normalized to sample weight to determine the specific low-field magnetic susceptibility (χ_{LF}). The low-field magnetic susceptibility is influenced to a minor extent by the amount of paramagnetic (e.g., clay minerals) and diamagnetic material (e.g., carbonates), and to a major extent by ferromagnetic *s.l.* material (e.g., magnetite or hematite in oxic shallow-water environments; Tarling and Hrouda, 1993).

Some representative samples were selected based on their χ_{LF} values with respect to the whole distribution and

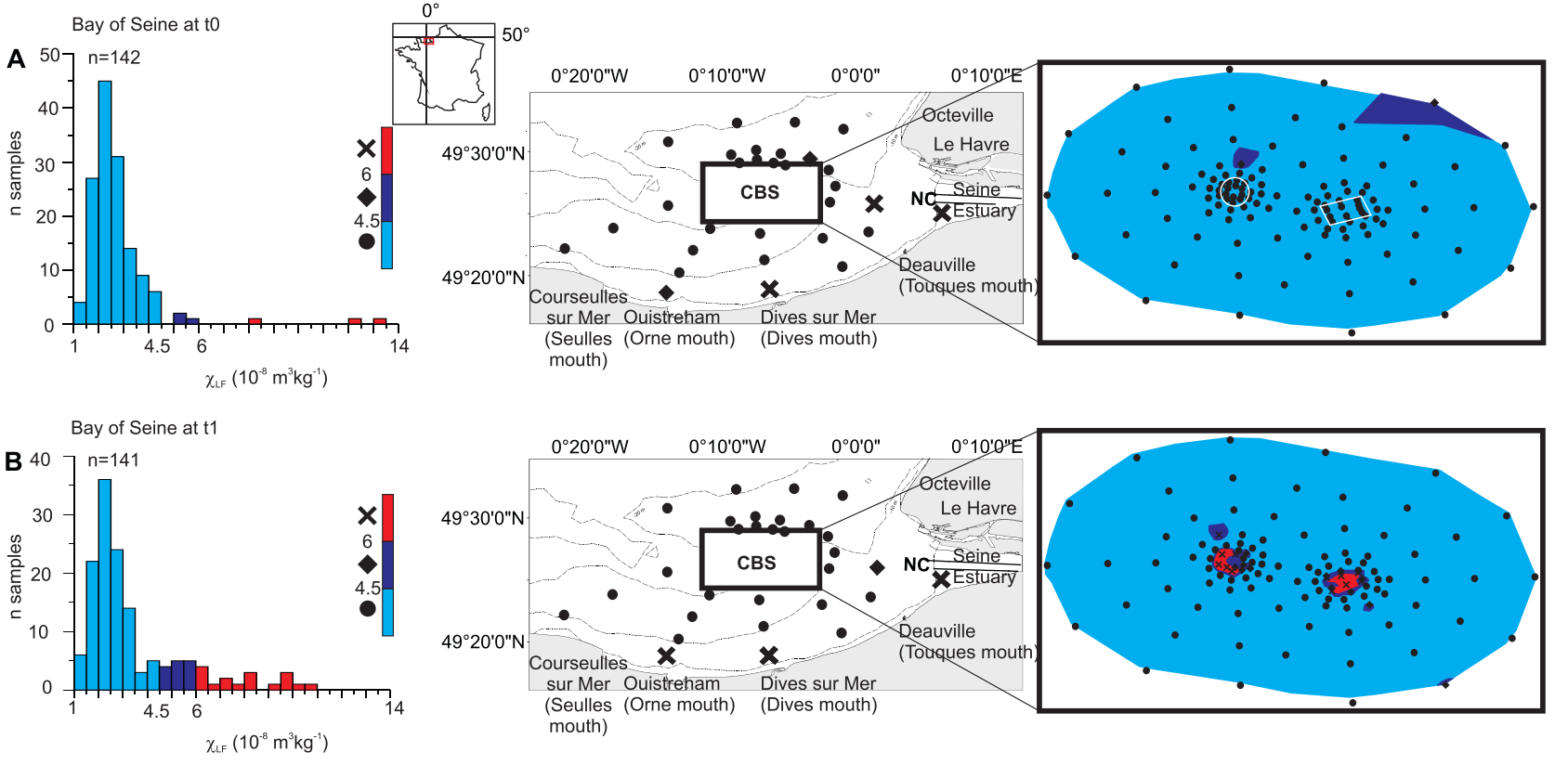

Fig. 1. A. Left: histogram of the distributions of the specific low-field magnetic susceptibility (χ_{LF}) grab sample values from the Bay of the Seine before dumping (t_0), displaying the number of samples for a $0.5{\cdot}10^{-8}$ m^3 kg^{-1} window. Centre: class map of the study area displaying the locations and χ_{LF} values of grab samples. Right: focus on the dispersal sites (CBS). The pictograms indicate the locations of the grab samples and their χ_{LF} values. The colour map results from a linear interpolation between the χ_{LF} grab sample values. The white circle and parallelogram indicate the dumping areas. B. Same as Fig. 1A, immediately after the last dumping (t_1).

depending on their geographic position to measure Anhysteretic Remanent Magnetization (ARM), Saturation Isothermal Remanent Magnetization (SIRM), and Isothermal Remanent Magnetization (IRM) using a superconducting rock magnetometer (2G enterprises, model SRM760R). The ARM device is a laboratory-induced magnetization gained in an alternating magnetic field of 100 mT superimposed on a constant steady field of 50 μT comparable to the strength of the geomagnetic field. The ARM is afterward subjected to demagnetization at 30 mT (i.e. ARM_{30}). The SIRM was acquired in a 3-T field and the IRM in a 0.3-T field in the opposite direction, both induced by pulse magnetizer MMPM9 (Magnetic Measurements Ltd.). The *S*-ratio was calculated using the formula $0.5 \times (1–IRM/SIRM)$, which allows for a potential estimation of the relative abundance of high-coercivity minerals (Bloemendal et al., 1992). The *S*-ratio is close to 1 when low-coercive minerals such as a magnetite dominate the signal, and decreases with increasing the amount of high-coercive minerals such as hematite (Bloemendal et al., 1992). The Hard Isothermal Remanent Magnetization (HIRM) was calculated using the formula (SIRM-IRM)/2 and allows for an estimation of the absolute concentration of high-coercivity minerals (e.g., hematite; Robinson, 1986).

Further detailed rock magnetic investigations were performed on 13 selected samples. From the dumping sites, a total of eight samples were chosen, i.e. two at t_0, t_1, t_2 and t_3. Two samples were selected from the NC to characterize the dredged-dumped material. For comparison, two samples were picked from the Seine estuary and one sample from the coastal area. Hysteresis loops and backfield curves were measured using a Vibrating Sample Magnetometer MicroMag 3900 (Lakeshore) to determine the magnetic characteristics of the samples. To estimate the contribution of paramagnetic particles to the low-field specific susceptibility signal, the slope of the linear component of the hysteresis loops expressed in $Am^2\,T^{-1}\,kg^{-1}$ was calculated and multiplied by the magnetic permeability of the free space (m_0) to determine the high-field specific susceptibility (χ_{HF}) expressed in $m^3\,kg^{-1}$. Stepwise thermal demagnetization of the SIRM acquired at 3 T was done using a MMTD80 oven (Magnetic Measurements Ltd.) to determine unblocking temperatures. Steps in thermal treatment are 25, 100, 150, 200, 250, 300, 350, 400, 450, 500, 550, 580 and 610 °C. In order to estimate the contribution of submicron-size superparamagnetic particles to the susceptibility signal and to the hysteresis loops, the frequency-dependence was determined from magnetic susceptibility measurements at 976 and 15616 Hz using a MFK1 AGICO susceptibilimeter (AGICO; data available on http://doi.pangaea.de/10.1594/PANGAEA.832049).

2.4. Non-magnetic proxies

2.4.1. Carbonate content

To assess the magnetic nature of the material that causes χ_{LF} variations, the carbonate content was measured on 36 samples displaying low χ_{LF} values. The carbonate content was determined using a Bernard calcimeter (Black et al., 1965). The determination of $CaCO_3$ is based on the volumetric analysis of the CO_2 that is liberated during the application of an HCl solution (10%) on 0.2 g of grounded homogenized sample. The process was repeated two to six times for each sample. The value displayed for each sample is thus an average of the two to six analyses.

2.4.2. Grain size measurements

The grain size distribution of 248 bulk sediment samples was analysed with a Beckman Coulter LS230 laser particle seizer at the M2C laboratory (Caen, France). The grain sizes were defined by volume percentage and the fraction < 63 μm (i.e. fine fraction) was calculated.

2.5. Interpolation method for map construction

An interpolation between data points was performed by using an exact interpolator in Surfer, Triangulation with Linear Interpolation so-called Delaunay triangulation (Surfer tutorials and references therein; http://www.goldensoftware.com/newsletter/issue71-surfer-gridding-methods-part1). Since our data are not evenly distributed over the grid area, data containing sparse areas result in distinct triangular facets on the map. To avoid misleading interpolations between distant points, interpolation was only used within a limited frame extending around the disposal sites (CBS).

3. Results

3.1. Specific low-field magnetic susceptibility (χ_{LF})

Before dumping, magnetic characterization of the sediments from the Bay of the Seine seafloor and from the NC was performed using the specific low-field magnetic susceptibility χ_{LF}. In order to assess the susceptibility background of the Bay of the Seine before dumping, the distribution of the 142 χ_{LF} values was plotted in a histogram displaying the number of samples for a $0.5{\cdot}10^{-8}\,m^3\,kg^{-1}$ window (Fig. 1A). The log-normal-shaped distribution ranged from 1 to $14{\cdot}10^{-8}\,m^3\,kg^{-1}$, with a modal value around 2 to $2.5{\cdot}10^{-8}\,m^3\,kg^{-1}$. The totality of the samples originating from the CBS showed values below $6{\cdot}10^{-8}\,m^3\,kg^{-1}$, with 98.4% of the CBS samples ranging from 1 to $4.5{\cdot}10^{-8}\,m^3\,kg^{-1}$, whereas the samples retrieved in the vicinity of the Orne and Dives rivers' mouths displayed values higher than $4.5{\cdot}10^{-8}\,m^3\,kg^{-1}$, and higher than $6{\cdot}10^{-8}\,m^3\,g^{-1}$ in the Seine estuary (Fig. 1A). Such high-susceptibility values reveal a terrestrial input restricted to coastal areas. It must be noted that no sampling station was located close enough to the Seulles and Touques river mouths to record the influence of the sediment discharge from these potential additional sources.

The NC sediments displayed χ_{LF} values ranging from 2.3 to $12.3{\cdot}10^{-8}\,m^3\,kg^{-1}$ (data available on http://doi.pangaea.de/10.1594/PANGAEA.830269). The dumped sediments were a mixture originating from the two dredging sites, which mean value was $\sim 6.5{\cdot}10^{-8}\,m^3\,kg^{-1}$ (the different dredging sites contributions of 47 and 53% did not influence the mean value). This NC mean value was

higher than all the pre-dumping CBS values and was comparable to the range of the samples retrieved in the Seine estuary (Fig. 1A). Therefore, the limit to which sediments were considered as dredged-dumped material was set to $6{\cdot}10^{-8}\,m^3\,kg^{-1}$. The limit at $4.5{\cdot}10^{-8}\,m^3\,kg^{-1}$ was used to account for the dilution of the dumping susceptibility signal in the background of the Bay of the Seine. These limits were then applied to datasets immediately after the last dumping in order to establish class maps for the studied area (Fig. 1B).

Immediately after the last dumping in February 2013, the distribution of the 141 samples from the Bay of the Seine exhibited a similar log-normal-shaped distribution to before dumping, with the difference that a larger number of samples showed χ_{LF} values above $6{\cdot}10^{-8}\,m^3\,kg^{-1}$ (Fig. 1B). Among those, three samples were retrieved in the vicinity of the river mouths of the Orne, the Dives, and the Seine, and the remaining high χ_{LF} values were located on the dumping areas. Whereas the three high-susceptibility values located on coastal areas were induced by the natural fluvial input, the rest of the high-susceptibility values that were located more offshore allowed for a monitoring of the dispersion of dumped sediments within the CBS area. Before dumping, CBS sediments showed values below $6{\cdot}10^{-8}\,m^3\,kg^{-1}$. In contrast, after dumping, CBS sediments at dispersal sites showed values higher than $6{\cdot}10^{-8}\,m^3\,kg^{-1}$ (Fig. 1B).

3.2. Magnetic mineralogy

The thermal demagnetization curves of the SIRM display a progressive and constant unblocking of the magnetization that reaches 0 at 550 °C (Fig. 2A). This demagnetization pattern is related to the predominance of poorly substituted titanomagnetite. A single sample retrieved at t_0 reaches 0 at 580 °C, which corresponds to the Curie temperature of pure magnetite. A sample from the NC shows a slight inflexion at around 450 °C induced by destabilization of a small quantity of maghemite. Magnetite and poorly substituted titanomagnetite dominate the SIRM signal in all 13 samples (Fig. 2A).

With rather constant demagnetization patterns and with frequency-dependant magnetic susceptibilities below 6% showing the low influence of superparamagnetic particles on the magnetic signal (data available on http://doi.pangaea.de/10.1594/PANGAEA.832049), hysteresis loops can be interpreted in terms of magnetic grain sizes. Characteristic parameters calculated from hysteresis loops after paramagnetic correction (Fig. 2B) and backfield curves indicate that the 13 samples are all displayed within a very narrow grain size range from 1 to 20 μm in pseudo-single domain area (PSD; Fig. 2C; Dunlop, 2002). Before dumping, samples from the Bay of the Seine, from the NC, and from the coast and the estuary are broadly distributed. Values for samples from the Bay of the Seine from t_1 to t_3 show a change toward fine magnetic grain sizes with time, as opposed to values at t_0 that show the most coarse grain sizes (Fig. 2C). This pattern is not consistent with a resilience that would lead to a data shift toward t_0 values with time. Consequently, hysteresis parameters that describe the entire spectrum of coercivity of the magnetic minerals comprised in the samples are not very sensitive to the dumping process: hysteresis parameters have a narrow range of variations and do not show a clear tendency, especially in terms of resilience.

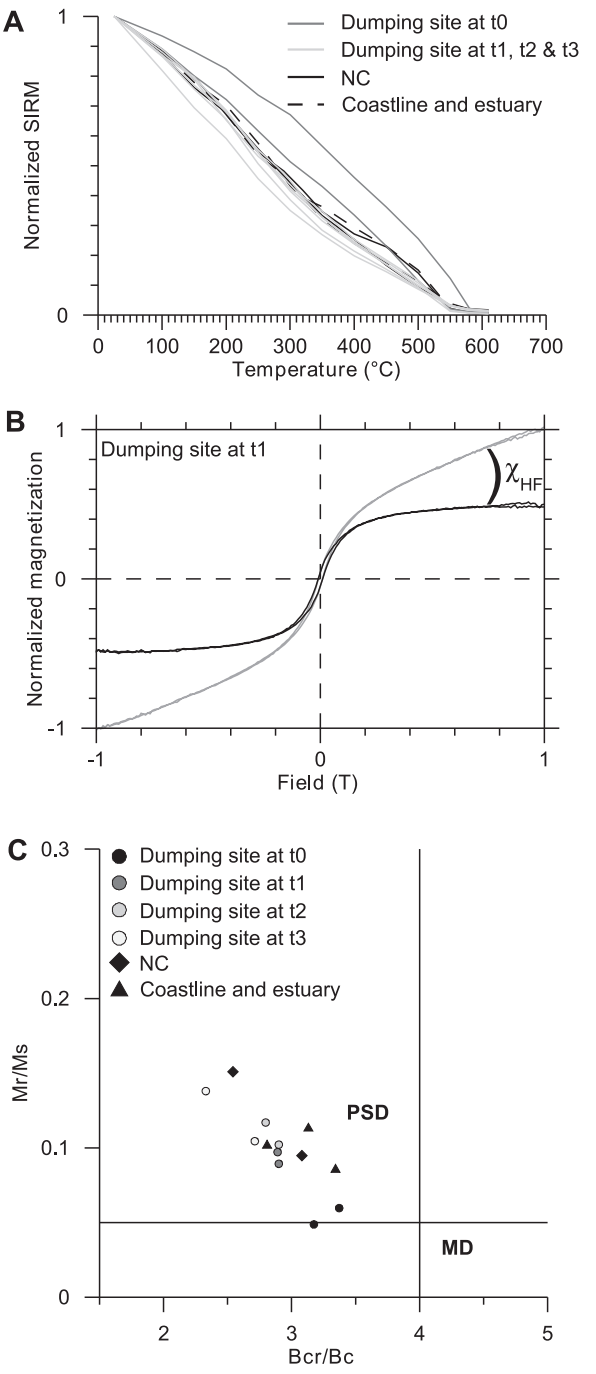

Fig. 2. A. Thermal demagnetization of the Saturation Isothermal Remanent Magnetization for 13 selected samples. B. Example of a hysteresis loop, the determination of the paramagnetic slope is used to calculate the high-field magnetic susceptibility (χ_{HF}). C. Ratio B_{cr}/B_c (coercive field of the remanence on coercive field) versus M_r/M_s (remanent magnetization on saturation magnetization). Pseudo-single domain (PSD) and multi-domain (MD) areas (Day et al., 1977) are displayed on the graph.

4. Discussion

4.1. Factors influencing the susceptibility signal

4.1.1. Bulk grain size vs. specific low-field magnetic susceptibility

The correlation between laser-based grain size and susceptibility was investigated by plotting the proportion of fine fraction ($< 63\,\mu m$) vs. χ_{LF} for samples located within the CBS. The NC samples showed a wide range of grain size distributions ranging from 0 to 66% of fine fraction, four samples displayed almost no fine fraction, whereas two samples showed $\sim$60% of fine fraction (Fig. 3A). The CBS before dumping showed low proportions of fine fraction with maximum values reaching 20% (Fig. 3B), whereas after dumping CBS exhibited grain sizes up to 66% of fine fraction (Fig. 3C). Those results exhibit an input of fine fraction sediments in the CBS by dumping. Before and after dumping, the plots of the proportion of fine fraction vs. χ_{LF} display a high-scattered pattern and, therefore, no linear relationship between the two parameters (Fig. 3B and C). The magnetic mineralogy shows that micrometric magnetite dominates the remanent signal. Furthermore, the magnetic susceptibility signal can be modulated by the concentration in ferromagnetic magnetite, which is in the order of few ppms, but also by paramagnetic clays and diamagnetic carbonates and quartz contributions (see discussion hereafter). Laser-based grain size analysis and magnetic susceptibility must be therefore considered as different but complementary methods for monitoring dredged-dumped sediments at sea.

4.1.2. Concentration parameters

To assess the influence of diamagnetic material on susceptibility, the carbonate content was plotted against χ_{LF} for 18 CBS samples before and after dumping (Fig. 3D and E). The mean carbonate content of the 18 samples spread across the studied area does not show any significant change before and after dumping. First-approximation calcite corrections to pure calcite ($-0.48{\cdot}10^{-8}\,m^3\,kg^{-1}$; e.g., Dunlop and Ozdemir, 1997) would range between -0.06 and $-0.20{\cdot}10^{-8}\,m^3\,kg^{-1}$, which is negligible in comparison to the values displayed in this study. Therefore, there is no need for correction of the susceptibility data with respect to the carbonate content. The mean carbonate content remains around 25% (which is in the range of the values found in the literature for the Bay of the Seine, e.g., Garnaud, 2003), whereas the mean susceptibility rises significantly from 2.3 to $3.2{\cdot}10^{-8}\,m^3\,kg^{-1}$ (Fig. 3D and E). No correlation was found between susceptibility and carbonate content values. Thus, the observed rise in susceptibility is not controlled by a decrease in diamagnetic material.

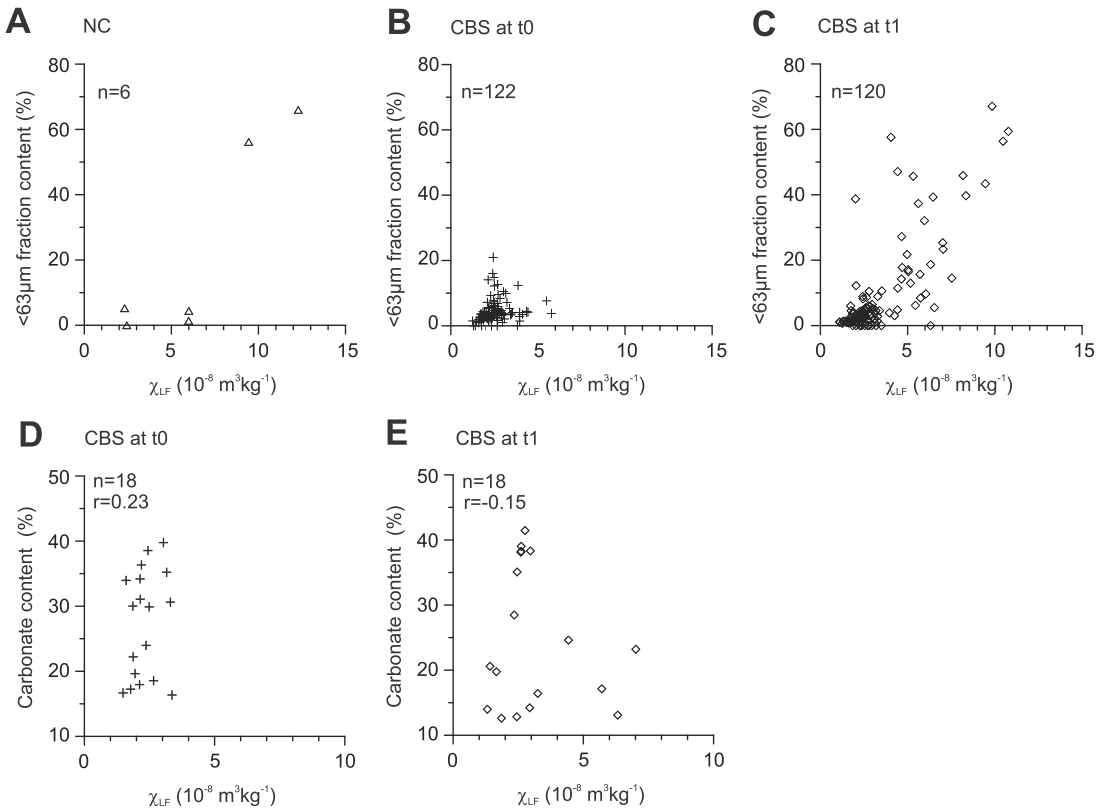

Fig. 3. A. Plot of the proportion of laser-based fine fraction ($< 63\,\mu m$) vs. specific low-field magnetic susceptibility (χ_{LF}) for grab samples retrieved in the navigation channel (NC). B. From the centre of the study area in the Bay of the Seine (CBS) before dumping (t_0). C. Immediately after the last dumping (t_1). D. Plot of the carbonate content vs. χ_{LF} for grab samples retrieved in the CBS at t_0. E. At t_1.

The magnetic nature of the material that enhances χ_{LF} values was investigated by plotting two parameters that are the SIRM (i.e. the ferromagnetic portion of the sediment) vs. χ_{LF} on NC and CBS samples. The NC shows SIRM values ranging from 2 to $13{\cdot}10^{-4}$ A m^2 kg^{-1} (Fig. 4A). Pre-dumping SIRM values for the CBS samples were centred between 1 and $5{\cdot}10^{-4}$ A m^2 kg^{-1} (except for a single value reaching $6{\cdot}10^{-4}$ A m^2 kg^{-1}; Fig. 4B). Post-dumping SIRM values covered a higher range and reached $7{\cdot}10^{-4}$ A m^2 kg^{-1} at t_1 (Fig. 4C). For the NC as well as for the CBS before and after dumping, the SIRM vs. χ_{LF} plots show positive linear trends with correlation coefficients around 0.98 (Fig. 4A–C). Therefore, the susceptibility signal is dominated by ferromagnetic particles.

To estimate the contribution of paramagnetic particles to the susceptibility signal, the high-field magnetic susceptibility χ_{HF}, carried by paramagnetic particles (when positive) and calculated from the paramagnetic slopes of the hysteresis loops (Fig. 2B), was calculated. The proportion of paramagnetic particles was then plotted against χ_{LF} for the 13 samples used for magnetic mineralogy (Fig. 4D). Whereas the χ_{LF} values display the differences described in Section 3.1, the magnetic susceptibility values measured for the paramagnetic particles do not show any particular trend. Paramagnetism contributes to 8–42% of magnetic susceptibility, but no correlation was found between paramagnetism and low-field magnetic susceptibility before and after dumping (Fig. 4D). The observed rise in susceptibility in the CBS is, thus, due to an input of ferromagnetic material by dumping.

4.2. Hysteretic and anhysteretic qualitative rock magnetic parameters

Isothermal remanent magnetization measurements show that the majority of *S*-ratio values approach 1, which indicates a relative high amount of low-coercive minerals (Bloemendal et al., 1992; i.e. magnetite according to the magnetic mineralogy; data available on http://doi.pangaea.de/10.1594/PANGAEA.830268). However, few *S*-ratio values approach 0.8, indicating a high proportion of highly coercive minerals (i.e. hematite or goethite). These results are in accordance with a comparison of HIRM to SIRM, which shows that high-coercive minerals contribute up to 18% of the SIRM signal for particular samples. Since the saturation magnetization of hematite is

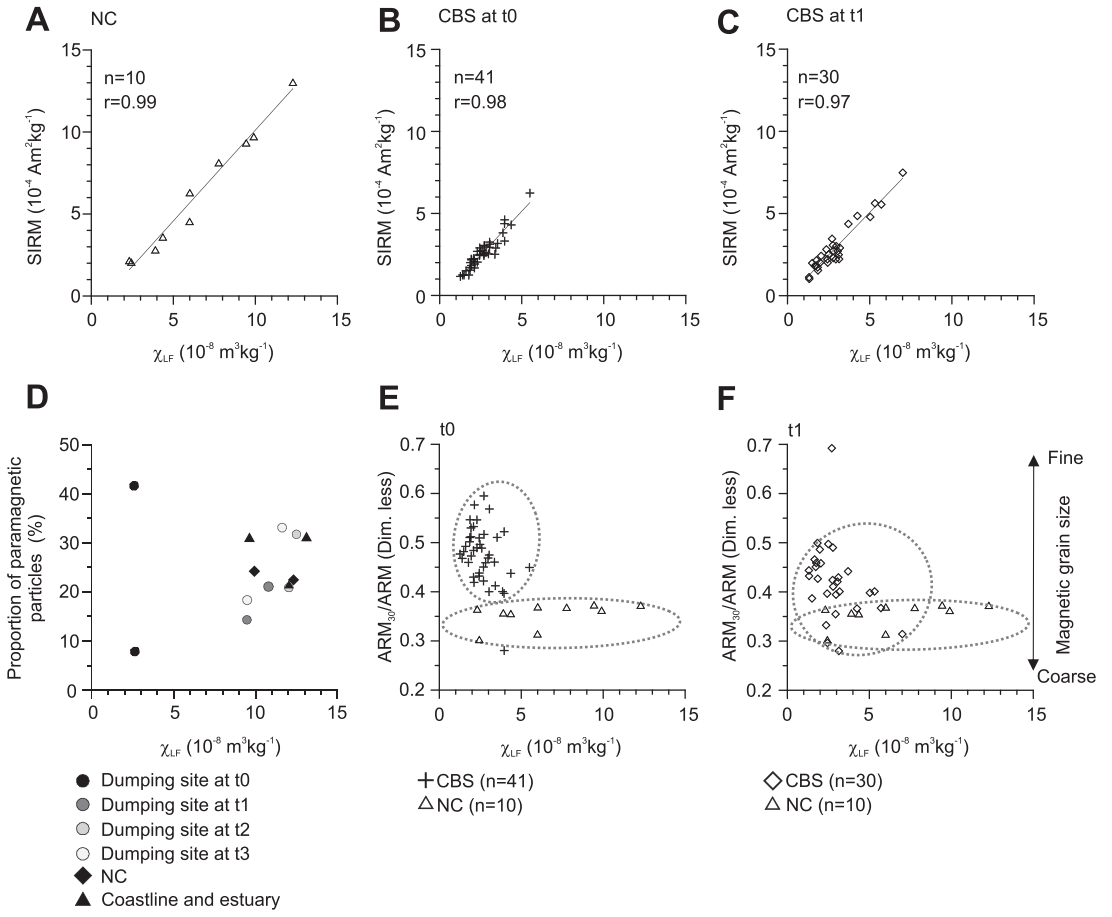

Fig. 4. A. Plot of the Saturation Isothermal Remanent Magnetization vs. specific low-field magnetic susceptibility (χ_{LF}) for grab samples retrieved in the navigation channel (NC). B. In the centre of the study area in the Bay of the Seine (CBS) before dumping (t_0). C. Immediately after the last dumping (t_1). D. Plot of the proportion of paramagnetic particles vs. χ_{LF} for the 13 samples selected for magnetic mineralogy. E. Plot of the Anhysteretic Remanent Magnetization $(ARM)_{30}$/ARM to χ_{LF} ratio for grab samples retrieved in the NC and in the CBS at t_0; 4F: at t_1.

200 times lower than that of magnetite (i.e. Walden, 1999), those peculiar samples may actually contain a dominant proportion of hematite. However, this high proportion of hematite does not affect their magnetic susceptibility, since magnetic susceptibility for hematite is 1000 times lower than for magnetite (i.e. Dearing, 1994).

The anhysteretic ratio ARM_{30}/ARM is more discriminating than the hysteretic parameters, *S*-ratio and HIRM, since it displays different values for NC and CBS at t_0 (Fig. 4E). The ARM_{30}/ARM vs. χ_{LF} plot clearly displays two distinct clouds. The CBS values range between 0.4 and 0.6 (with the exception of one single data point), whereas NC values lie below 0.37. At t_1, the CBS values decrease to 0.25 to 0.5 (with exception to one single data point), which corresponds to the range of the NC values (Fig. 4F). In the Bay of Seine, Sorrel et al. (2009) have been using ARM_{30}/ARM as a downcore coercivity parameter. However, for samples having a constant mineralogy dominated by magnetite, as it is the case for our surface samples, ARM_{30}/ARM may be used as a magnetic grain size estimator (Johnson et al., 1975) for the low-coercive fraction. The shift of CBS values towards NC values after dumping reveals an input of coarser low-coercive magnetic grains compared to the background signal (Fig. 4F). This magnetic grain size change is the signature of NC sediments input in the Bay of Seine caused by dumping.

4.3. Resilience of the Bay of Seine sedimentary environment

4.3.1. Evolution of the magnetic susceptibility

Magnetic susceptibility distributions in the Bay of Seine were examined during a 6-month period after the last dumping (Fig. 5A). The three post-dumping distributions of ~ 142 χ_{LF} values from the Bay of Seine displayed similar log-normal-shaped distributions with minor differences. The proportions of χ_{LF} values above $6{\cdot}10^{-8}\,m^3\,kg^{-1}$ remained stable (i.e. $\sim 11\%$ of the samples) due to the input of high-susceptibility sediments from the continent (data available on http://doi.pangaea.de/10.1594/PANGAEA.830175). These results outline the natural (i.e. not linked to dumping activities) non-conservative character of the Bay of Seine sedimentary system. Thus, these histograms of distributions are only relevant when combined together with the spatial monitored data.

The monitoring of the χ_{LF} values through the defined class maps allows us to record: (1) the terrestrial input; (2) the dispersion of dumped sediments over the CBS (Fig. 5A). Only the map of September 2013 showed high-susceptibility inputs from the Seine River. Low Seine river runoff was recorded (data available on http://seine-aval.crihan.fr/web/pages.jsp?currentNodeId=150), which is commonly the case in this season (Lesourd et al., 2003). This input might be the result of the sedimentary regime prevailing in the Bay of Seine. During winter, mud accumulation takes place in the proximal outlet part of the estuary, while during low river runoff, the available mud is reworked by waves and tidal currents and scattered away offshore (Lesourd et al., 2003).

After dumping, both sites display χ_{LF} values $> 6{\cdot}10^{-8}\,m^3\,kg^{-1}$ (Fig. 5A). Deposits appear in the form of patches, when monitored on the maps immediately after dumping. Three months after the last dumping, dumped sediments remained in the form of patches, with a higher dilution of the susceptibility signal on the eastern dumping site. Six months after dumping, the eastern dumping site showed susceptibility values $< 6{\cdot}10^{-8}\,m^3\,kg^{-1}$. However, the decrease did not reach pre-dumping values. The western site still displayed patches of sediments with high-susceptibility values. Such different dilution trends might be due to the different dumping techniques.

Downcore χ_{LF} fluctuations were measured on four 12-cm long Reyneck box cores (Fig. 5B). Downcore variations are low and for each sampling station χ_{LF} values are similar to the ones measured on the samples retrieved with the Shipek grab. Such findings account for a negligible resuspension during sampling. The low-dispersion trend observed with grab samples at t_2 is also supported by the core data. Cores originating from the centre of the dumping sites (i.e. sampling stations 51 and 78) show variations before and after dumping, whereas stations 24 and 108, which are located ~ 1.9 km north and south of the dumping sites, do not display any remarkable change (Fig. 5B). Samples originating from the centre of dumping areas show variations of susceptibility values that display the following pattern: low values before dumping, an increase during dumping that reaches a maximum immediately after the last dumping, and finally a decrease towards pre-dumping values. This observation accounts for a low remobilization of the sediment up to 2 months after dumping.

4.3.2. Evolution of the dumping-sensitive magnetic parameter ARM_{30}/ARM

The sedimentary evolution of the Bay of the Seine was monitored during a 6-month period using the magnetic grain size parameter ARM_{30}/ARM (Fig. 5C). The distributions of the ARM_{30}/ARM values from the CBS were organized in a histogram displaying the number of samples for a window of 0.05. As discussed in Section 4.2, initial NC and CBS values were well constrained with mean values at respectively 0.35 and 0.47 and modal values respectively around 0.35 to 0.40 and 0.45 to 0.50. Immediately after the last dumping, CBS distribution values shifted towards NC values with a mean of 0.42, and modal values around 0.40 to 0.45. Three to 6 months after the last dumping whereas mean and modal values remained steady, their distributions showed a partial resilience with an increasing amount of samples reaching values between 0.45 and 0.55.

A modification of the sedimentary environment of the CBS by an input of dredged-dumped sediments is observed using the magnetic grain size parameter ARM_{30}/ARM and partly persists even 6 months after dumping. This interpretation might suffer from two main biases that are: (1) a too low sampling choice among the CBS stations; (2) non-conservative sedimentary system due to terrestrial input. Nevertheless, low-field magnetic susceptibility and anhysteretic magnetic parameters indicate that mineralogical resilience of the CBS seafloor is in progress. A longer survey would allow for a better evaluation of the on-going resilience pattern.

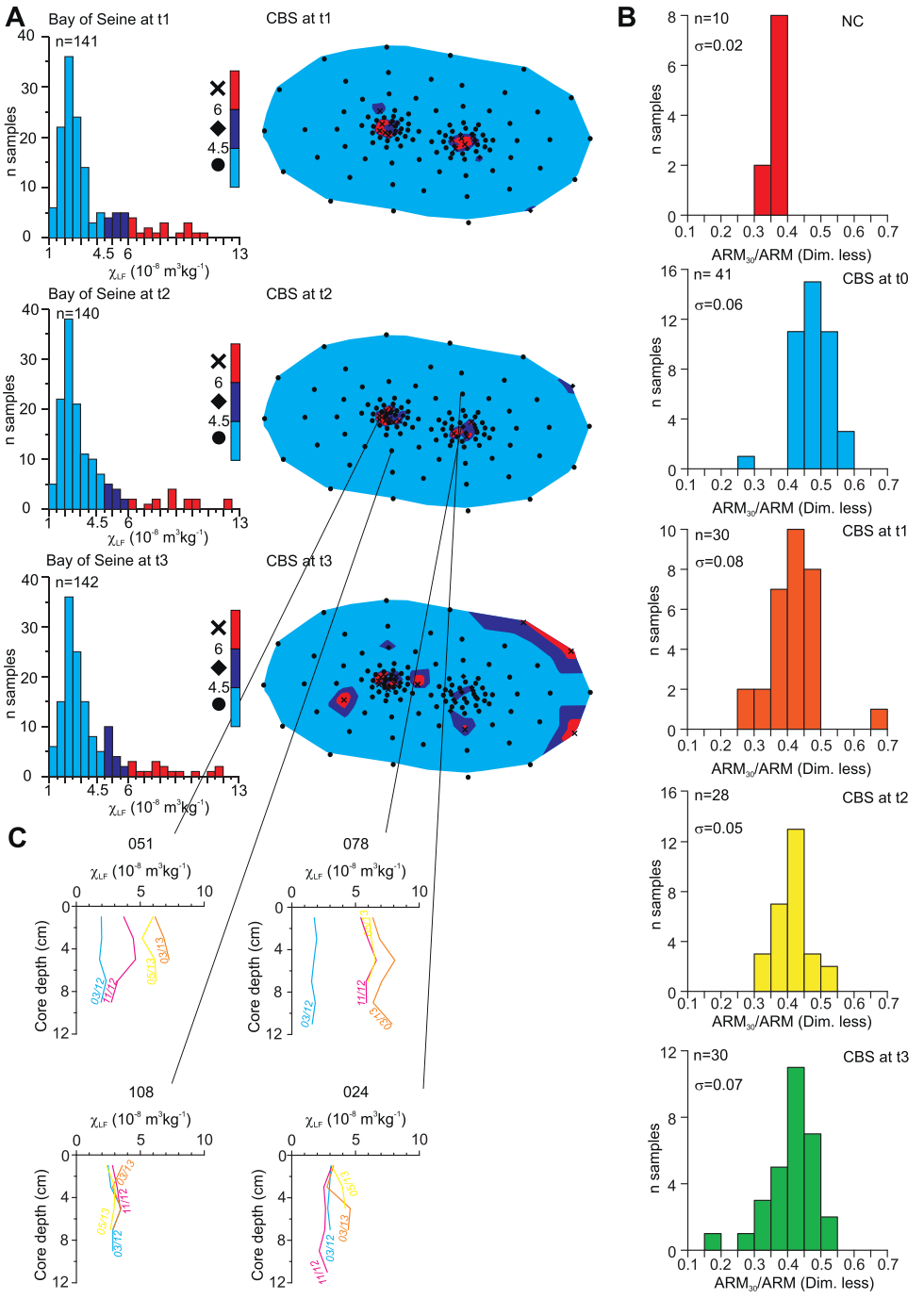

Fig. 5. A. Left: histograms of the distributions of the specific low-field magnetic susceptibility (χ_{LF}) grab sample values from the Bay of the Seine (CBS) displaying the number of samples for a $0.5{\cdot}10^{-8}$ m^3 kg^{-1} window. Right: locations and χ_{LF} values of grab samples in the CBS zone (pictograms), and linear interpolation between the χ_{LF} data points (colour map) immediately (t_1), 3 months (t_2) and 6 months (t_3) after dumping. B. Histograms of the distributions of the Anhysteretic Remanent Magnetization $(ARM)_{30}$/ARM values displaying the number of samples for a 0.05 window for samples retrieved in the navigation channel (NC) and in the CBS before (t_0), immediately (t_1), 3 (t_2) and 6 months (t_3) after the last dumping. C. Downcore χ_{LF} fluctuations measured on four cores originating from the centre of the dumping sites (i.e. sampling stations 78 and 51) and located ~ 1.9 km to the north and south (i.e. sampling stations 24 and 108). Dates of the retrieval are displayed.

5. Conclusions

Our rock magnetism study shows that discrete magnetic susceptibility measurements are a fast and efficient tool for mapping the dispersion of dredged-dumped sediments at the seafloor and evaluate the subsequent resilience of the sedimentary environment. Dredged sediments originating from the navigation channel of the Seine River exhibit higher susceptibilities than the natural sedimentary background of the Bay of the Seine. Therefore, fingerprinting and monitoring the dispersion of the dumped sediments was possible over a 6-month survey. Besides, the influence of terrestrial input was also detected in our susceptibility maps but restricted to coastal areas.

Grain size trend analysis is a commonly used method to study sediment transport at a disposal site (e.g. Friend et al., 2006; Okada et al., 2009). Grain size trend analysis methods assume that distributions tend to approximate statistical normality or log-normality, but our navigation channel and Bay of the Seine natural sediment samples show polymodal particle-size distributions, introducing thus an inevitable loss of information (Forrest and Clark, 1989). Therefore, magnetic susceptibility must be considered as a complementary method to grain size analysis for monitoring dredged-dumped spoils at sea.

To comprehend the nature of the magnetic susceptibility signal, an analysis of the magnetic mineralogy of the sediment was performed. The susceptibility signal was found to be controlled by ferromagnetic particles. This investigation also revealed a constant magnetic mineralogy carried by pseudo-single domain magnetite particles before and after dumping. Among all the remanent magnetic parameters, the anhysteretic magnetic parameter ARM_{30}/ARM was the most discriminating. In a frame of constant magnetic mineralogy, this parameter can be used as grain size indicator for the low-coercive magnetic fraction. It allowed us to decipher the dredged-dumped sediments from the sedimentary background and to estimate its dilution during the resilience.

Magnetic parameters show that a 6-month survey was not sufficient to observe a complete resilience of the sedimentary system of the Bay of the Seine. A longer survey, combining magnetism and chemistry would be needed to determine the origin and the long-term evolution of the magnetic signal in the Bay of Seine for future dumping activities.

Acknowledgements

This study was funded by the "Grand Port Maritime de Rouen". It is an outcome of the CNRS and the University of Caen Basse-Normandie. We would like to acknowledge Jean-Claude Dauvin for providing laboratory facilities. We thank Pierre Rochette, Patrick Lesueur, Patrice Tournier, and Albert Gallicher for their support and useful discussions. Coralie Thouroude is acknowledged for her participation in the grain size measurements. The authors are grateful to the two reviewers, Christine Franke and Christian Crouzet, for their very useful comments and suggestions.

References

Akinyemi, F., Hutchinson, M., Mîndrescu, M., Rothwell, J., 2012. Lake sediment records of atmospheric pollution in the Romanian Carpathians. Quat. Int. 293, 1040–6182.

Avoine, J., Allen, G.P., Nichols, M., Salomon, J.C., Larsonneur, C., 1981. Suspended-sediment transport in the Seine estuary, France: effect of man-made modifications on estuary-shelf sedimentology. Mar. Geol. 40, 119–137.

Black, C.A., Evans, D.D., Dinauer, R.C., 1965. Methods of Soil Analysis, Part 1, Physical and Mineralogical Properties, Including Statistics of Measurement and Sampling, Monograph No. 9. American Society of Agronomy, Madison, Wisconsin, USA (770 p.).

Bloemendal, J., King, J.W., Hall, F.R., Doh, S.J., 1992. Rockmagnetism of Late Neogene and Pleistocene deep-sea sediments relationship to sediment source, diagenetic processes, and sediment lithology. J. Geophys. Res. 97, 4361–4375.

Boyd, S.E., Limpenny, D.S., Rees, H.L., Cooper, K.M., Campbell, S., 2003. Preliminary observations of the effects of dredging intensity on the re-colonisation of dredged sediments off the southeast coast of England (Area 222). Estuarine, Coastal Shelf Sci. 57, 209–223.

Chevreuil, M., Blanchard, M., Teil, M.J., Chesterikoff, A., 1998. Polychlorobiphenyl behaviour in the water/sediment system of the Seine river, France. Water Res. 32, 1204–1212.

Chiffoleau, J.-F., Auger, D., Chartier, E., 1999. Fluxes of selected trace metals from the Seine estuary to the eastern English Channel during the period August 1994 to July 1995. Cont. Shelf Res. 19, 2063–2082.

Cooper, K., Boyd, S., Eggleton, J., Limpenny, D., Rees, H., Vanstaen, K., 2007. Recovery of the seabed following marine aggregate dredging on the Hastings Shingle Bank off the southeast coast of England. Estuarine, Coastal Shelf Sci. 75, 547–558.

Day, R., Fuller, M., Schmidt, V.A., 1977. Hysteresis properties of titanomagnetites grain size and compositional dependence. Phys. Earth Planet. Inter. 13, 260–267.

Dearing, J.A., 1994. Environmental Magnetic Susceptibility: Using the Bartington MS2 System. Chi Publishing, Kenilworth, UK104.

Du Four, I., Van Lancker, V., 2008. Changes of sedimentological patterns and morphological features due to the disposal of dredge spoil and the regeneration after cessation of the disposal activities. Mar. Geol. 255, 15–29.

Dunlop, D.J., 2002. Theory and application of the Day plot (Mrs/Ms versus Hcr/Hc). 1. Theoretical curves and tests using titanomagnetite data. J. Geophys. Res. 107 , http://dx.doi.org/10.1029/2001JB000487.

Dunlop, D.J., Ozdemir, O., 1997. Rock Magnetism: Fundamentals and Frontiers. Cambridge University Press, New York, London and Cambridge (573 p.).

Fettweis, M., Baeye, M., Francken, F., Lauwaert, B., Van den Eynde, D., Van Lancker, V., Martens, C., Michielsen, T., 2011. Monitoring the effects of disposal of fine sediments from maintenance dredging on suspended particulate matter concentration in the Belgian nearshore area (southern North Sea). Mar. Pollut. Bull. 62, 258–269.

Forrest, J., Clark, N.R., 1989. Characterizing grain size distribution: evaluation of a new approach using a multivariate extension of entropy analysis. Sedimentology 36, 711–722.

Franke, C., Kissel, C., Robin, E., Bonté, P., Lagroix, F., 2009. Magnetic particle characterization in the Seine river system: implications for the determination of natural versus anthropogenic input. Geochem. Geophys. Geosyst. 10 , http://dx.doi.org/10.1029/2009GC002544.

Friend, P.L., Velegrakis, A.F., Weatherston, P.D., Collins, M.B., 2006. Sediment transport pathways in a dredged ria system, Southwest England. Estuarine, Coastal Shelf Sci. 67, 491–502.

Garnaud, S., 2003. La sédimentation fine sur une plate-forme interne actuelle macrotidale : la baie de Seine sud-orientale (France) (Ph.D. Thesis). (308 p.).

Horng, C.S., Huh, C.A., Chen, K.H., Huang, P.R., Hsiung, K.H., Lin, H.L., 2009. Air pollution history elucidated from anthropogenic spherules and their magnetic signatures in marine sediments offshore of southwestern Taiwan. J. Mar. Syst. 76, 468–478.

Johnson, H.P., Lowrie, W., Kent, D.V., 1975. Stability of anhysteretic remanent magnetization in fine and coarse magnetite and maghemite particles. Geophys. J. R. Ask. Soc. 41, 1–10.

Lepland, A., Bøe, R., Lepland, A., Totland, O., 2009. Monitoring the volume and lateral spread of disposed sediments by acoustic methods, Oslo Harbor, Norway. J. Environ. Manage. 90, 3589–3598.

Lesourd, S., Lesueur, P., Brun-Cottan, J.C., Garnaud, S., Poupinet, N., 2003. Seasonal variations in the characteristics of superficial sediments in a macrotidal estuary (the Seine inlet, France). Estuarine, Coastal Shelf Sci. 58, 3–16.

Li, M., Parrott, Z., Russell, D., Zongyan, Y., 2009. Sediment stability and dispersion at the Black Point offshore disposal site, Saint John Harbour, New Brunswick, Canada. J. Coastal Res. 25, 1025–1040.

McCubbin, D., Leonard, K.S., Maher, B.A., Hamilton, E.I., 2000. Association of ^{210}Po(^{210}Pb), $^{239+240}$Pu and ^{241}Am with different mineral fractions of a beach sand at Seascale, Cumbria, UK. Sci. Total Environ. 254, 1–15.

Meybeck, M., Lestel, L., Bonté, P., Moilleron, R., Colin, J.L., Rousselot, O., Hervé, D., de Pontevès, C., Grosbois, C., Thévenot, D.R., 2007. Historical perspective of heavy metals contamination (Cd, Cr, Cu, Hg, Pb, Zn) in the Seine River basin (France) following a DPSIR approach (1950–2005). Sci. Total Environ. 375, 204–231.

Okada, T., Larcombe, P., Mason, C., 2009. Estimating the spatial distribution of dredged material disposed of at sea using particle-size distributions and metal concentrations. Mar. Pollut. Bull. 58, 1164–1177.

Pozza, M.R., Boyce, J.I., Morris, W.A., 2004. Lake-based magnetic mapping of contaminated sediment distribution, Hamilton Harbour, Lake Ontario, Canada. J. Appl. Geophys. 57, 23–41.

Roberts, D.A., 2012. Causes and ecological effects of resuspended contaminated sediments (RCS) in marine environments. Environ. Int. 40, 230–243.

Robinson, S.G., 1986. The Late Pleistocene palaeoclimatic record of North Atlantic deep-sea sediments revealed by mineral-magnetic measurements. Phys. Earth Planet. Inter. 42, 22–47.

Roy, S., Gaillardet, J., Allègre, C.J., 1999. Geochemistry of dissolved and suspended loads of the Seine river, France: anthropogenic impact, carbonate and silicate weathering. Geochim. Cosmochim. Acta 63, 1277–1292.

Sorrel, P., Tessier, B., Demory, F., Delsinne, N., Mouazé, D., 2009. Evidence for millennial-scale climatic events in the sedimentary infilling of a macrotidal estuarine system, the Seine estuary (NW France). Quat. Sci. Rev. 28, 499–516.

Tarling, D.H., Hrouda, F., 1993. The Magnetic Anisotropy of Rocks. Chapman and Hall, London (217 p.).

Van der Wal, D., Forster, R.M., Rossi, F., Hummel, H., Ysebaert, T., Roose, F., Herman, P.M.J., 2011. Ecological evaluation of an experimental beneficial use scheme for dredged sediment disposal in shallow tidal waters. Mar. Pollut. Bull. 62, 99–108.

Venema, L.B., de Meijer, R.J., 2001. Natural radionuclides as tracers of the dispersal of dredge spoil dumped at sea. J. Environ. Radioact. 55, 221–239.

Venkatachalapathy, R., Veerasingam, S., Basavaiah, N., Ramkuma, T., Deenadayalan, K., 2011. Environmental magnetic and petroleum hydrocarbons records in sediment cores from the North-East coast of Tamilnadu, Bay of Bengal, India. Mar. Pollut. Bull. 62, 681–690.

Verney, R., Deloffre, J., Brun-Cottan, J.C., Lafite, R., 2007. The effect of wave-induced turbulence on intertidal mudflats: impact of boat traffic and wind. Cont. Shelf Res. 27, 594–612.

Walden, J., 1999. Remanence measurements. In: Walden, J., Oldfield, F., Smith, J. (Eds.), Environmental Magnetism: A Practical Guide, Technical Guide No. 6. Quaternary Research Association, London, pp. 63–88.

Wienberg, C., Bartholomä, A., 2005. Acoustic seabed classification in a coastal environment (outer Weser Estuary, German Bight) a new approach to monitor dredging and dredge spoil disposal. Cont. Shelf Res. 25, 1143–1156.

Yang, D., Zheng, L., Song, W., Chen, S., Zhang, Y., 2012. Evaluation indexes and methods for water quality in ocean dumping areas. Proc. Environ. Sci. 16, 112–117.